Correlative multi-spectroscopic and microscopic analyses for investigation of UV-C QDs bimodal emission

Dr. Adeline Grenier[1], Dr. Jesus Canaz[2], Mrs Névine Rochat[1], Dr. Zineb Saghi[1], Dr. Jean-Luc Rouvière[3], Dr. Edith Bellet-Almaric[2], Mrs. Audrey Jannaud[1], Dr. Anjali Harikumar[2], Dr. Catherine Bougerol[4], Dr. Lorenzo Rigutti[5], Dr. Eva Monroy[2]

[1]Univ. Grenoble Alpes, CEA, Leti, F-38000 Grenoble, Grenoble, France, [2]Univ. Grenoble-Alpes, CEA, Grenoble INP, IRIG, PHELIQS, 38000 Grenoble, France,, Grenoble, France, [3]Univ. Grenoble Alpes, CEA, IRIG, MEM, 38000 Grenoble, France, grenoble, France, [4]Univ. Grenoble Alpes, CNRS, Grenoble INP, Institut Neel, 38000 Grenoble, France, Grenoble, France,

[5]UNIROUEN, CNRS, Groupe de Physique des Matériaux, Normandie Université, 76000 Rouen,France, Grenoble, France

Background and aims

There is a strong interest in the development of efficient solid-state UV-C sources in the 220-270 nm range due to their powerful germicidal properties. Light emitting diodes (LEDs) based on the AlGaN semiconductor system are the most promising approach, but the early stage of development of the AlGaN technology still presents challenges, such as inefficient p-type doping and resistive ohmic contacts, resulting in low efficiencies. An approach that circumvents these material limitations is the use of electron beam pumped lamps; with a UV-emitting material (anode) housed in a vacuum tube. High-energy electrons are emitted from a cold cathode and accelerated towards the semiconductor anode, generating free carriers. Unlike LEDs, electron beam pumped lamps don't require p-type doping or contacts. To further enhance device performance, the use of AlGaN quantum dots (QDs) as radiative recombination centers is very promising. The three-dimensional (3D) carrier confinement within QDs prevents carrier diffusion towards non-radiative centers, leading to improved radiative efficiency even at high temperatures. However, samples emitting at wavelengths shorter than 270 nm present broad or bimodal spectra. It is crucial to minimize bimodal emission or emission line width to achieve highly efficient devices for disinfection.
In this work, we investigate the origin of the bimodal emission in Al0,14Ga0,86N/AlN QD superlattices designed for electron beam pumped UV emitters. We propose a comprehensive analysis combining 2D-3D scanning transmission electron microscopy (STEM), atom probe tomography (APT), cathodoluminescence (CL) spectroscopy associated to 3D simulations of the electronic structure.

Methods

The sample consists of 100 periods of Al0,14Ga0,86N/AlN self-assembled Stranski-Krastanov QDs deposited on commercial 1-µm-thick (0001)-oriented AlN-on-sapphire templates by plasma assisted molecular beam epitaxy (MBE) [Fig.1(b)]. 2D and 3D structural properties of the samples were studied by bright field (BF) and high-angle annular dark field (HAADF) STEM imaging using a probe-corrected Titan Themis (Thermo Fisher Scientific) operating at 200 kV. Compositional information of the sample was measured by laser-assisted atom probe tomography using a CAMECA FlexTAP instrument. Cathodoluminescence measurements were carried out using an Attolight CL-dedicated SEM microscope. The electronic structure of the QDs was modelled using the Nextnano3 8-band k·p Schrödinger-Poisson equation solver with AlN and GaN parameters and experimental dimensions and composition as inputs parameters.

Results

The top-view CL [fig.2(a)] presents a predominant line at 290 nm and a secondary emission at 305 nm. The SEM (scanning electron microscopy) image associated to the λ-filtered CL map [Fig.2(b)] evidences that the emission at longer wavelengths is linked to pits.

To gain deeper understanding of the structural and optical effects associated with the pits observed at the surface, we performed CL and transmission electron microscopy (TEM) characterization on the same TEM sample. Figure 3(a) presents a λ-filtered CL map of a zoomed region with two wavelength emission domains superimposed to a HAADF-STEM image of the same region. The associated HAADF-STEM image [Fig. 3(b)] shows that the longer wavelength emission appears associated with 3D conical structures.The zoomed BF-STEM image ([fig.3(c)] of a conical structure shows that it appears at the interface between the AlN buffer layer and the superlattice with inclined facets around 30° with the (0001) plane at the edge. To gain further insight into the nature and compostion of the conical domains, electron tomography has been performed and shows the propagation of the shallow pit profile through the superlattice [Fig.4(a)], with a brighter chemical-related contrast indicating a higher Ga content compared to the surrounding regions. In addition, HAADF-HRTSEM has allowed to determine the dimension of QDs in conical and homogeneous (non conical) emission regions.

APT was performed to gain combined 3D structural and quantitative compositional information within the conical structure. Figure 4(b) displays an APT Ga map; which enables the visualization of the QD planes, as they are those containing Ga. The upper part of the tip exhibits a homogeneous region with flat QD planes. However, a significant portion of the tip contains a threading defect which corresponds to the faceted step present at the boundary of the cone-shaped extended defect. Focusing on the APT analysis of 5 QD planes [Fig. 4(c)] located on the lower part of the sample, the Ga-atom planes exhibit a bending angle of approximately 30°, corresponding to the behavior observed in bright field (BF) STEM [Fig.4(d)]. Projected side and top view Ga map density for the 5 QD layers are presented in the figure 4(e) and (f), respectively. We see that the QD layers exhibit a Ga enrichment towards the 30° facet. We choose to quantify the composition of the QD-SL in the defect and homogenous region by the comparison of the Ga density. Considering that the non-defective regions contain Al0.14Ga0.86N QDs (nominal concentration deduced from growth conditions), we deduce that the faceted region should contain Al0.07Ga0.93N QDs, which should red shift the emission wavelength.

To investigate whether the chemical and morphological changes of the QD population within the entire structure are responsible for the emission bimodality, we conducted 3D simulations of the electronic structure of AlGaN/AlN QDs by solving the Poisson and Schrödinger equations using Nextnano3 within the conical and homogeneous regions. Dimensions and composition in (i) homogeneous [Fig.5 (a)], (ii) conical area [Fig.5 (b)] and (iii) at the frontier of the defect area with 30°-facet [Fig.5 (c)] are used as inputs parameters for simulations. The direct comparison between simulated and experimental wavelength in both regions [Fig. 5(d)] confirms that the bimodality emission is due to the different size and chemistry of the dots within the defect and at the defect boundary.

Conclusion

The bimodal emission is attributed to the presence of a secondary population of quantum dots located within cone-like structural defects. These defects emerge at the initial interface between the AlN buffer layer and the QD superlattice and propagate vertically. They are associated to a dislocation featuring a strong strain field, thereby facilitating the generation of a shallow pit characterized by 30° faceted boundaries.

Graphic:

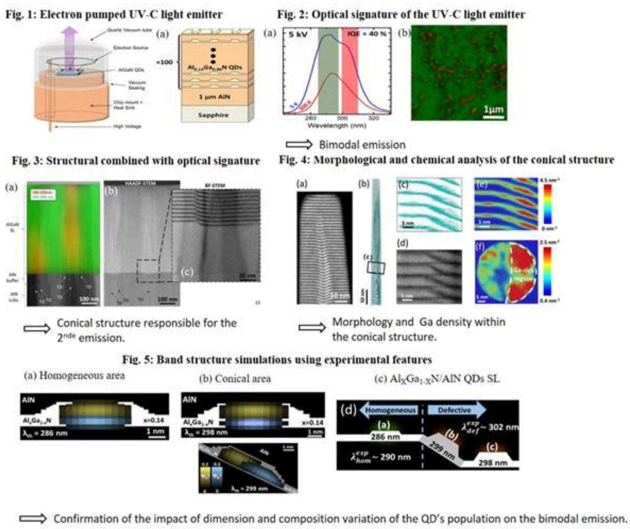

Keywords:

UV-QDs, bimodal emission, correlative microscopy

Reference:

[1]: J. Canaz et al., under review, ACS NANO.
[2]: This work, performed on the Platform for Nanocharacterisation (PFNC), was supported by the “Recherche Technologique de Base” and "France 2030 - ANR-22-PEEL-0014" programs of the French National Research Agency (ANR).
[3]: This project received funding from the French National Research Agency via the ASCESE-3D and FUSSL projects (ANR-21-CE50-0016 and ANR-22-CE09-0024).